Inkjet-Printed Wideband Planar Monopole Antenna on Cardboard for RF Energy-Harvesting Applications

Hossein Saghlatoon, *Member, IEEE*, Toni Björninen, *Member, IEEE*, Lauri Sydänheimo, *Member, IEEE*, Manos M. Tentzeris, *Fellow, IEEE*, and Leena Ukkonen, *Member, IEEE*

***Abstract*—We present a fully inkjet-printed novel wideband planar monopole antenna on thin packaging cardboard available in bulk for low-cost and environmentally-friendly mass manufacturing. We outline the characterization and the dielectric properties of the cardboard that are imperative for the successful design of an antenna on a paper-based substrate. To achieve highly conductive inkjet-printed pattern on the fibrous and porous cardboard, we deposit thin dielectric coating on the cardboard in the same inkjet process. The operation of the antenna is attested through simulations and measurements in the frequency range of 600–1500 MHz, where there are several strong radio signals present for ambient RF energy harvesting.**

***Index Terms*—Energy harvesting, inkjet printing, printable electronics, wideband planar monopole antenna.**

I. Introduction

MATERIAL choices in wireless devices have a huge impact on the environment, and presently the use of renewable, environmental-friendly materials and additive manufacturing methods, such as inkjet printing, is a growing trend. Great potential lies in the use of wood and paper as green platforms for antennas in ambient power harvesting, wireless sensor networks (WSNs), and radio frequency identification (RFID) [1]–[3]. As the lifetime of the batteries is a major aspect in the development of mobile wireless devices, various methods have been studied to reduce the power consumption and to increase the capacity of batteries [4]–[6]. On the other hand, energy harvesting using, e.g., piezoelectric transducers, solar cells, and ambient radio frequency (RF) sources provides compelling means for battery-free devices where the RF energy is stored temporarily in an energy reservoir such a supercapacitor [7]–[9].

In this letter, we focus on the design and inkjet-printing fabrication of a wideband planar monopole antenna on thin packaging cardboard available in bulk for low-cost and environmentally-friendly mass manufacturing. However, due to the porosity and high surface roughness, these types of materials are challenging platforms for inkjet printing. The ink droplets are easily absorbed in the platform, preventing the nanoscale metal particles contained in the ink from forming a pattern with high conductivity. To remedy this, an inkjet materials printer can be utilized to pretreat the platform with a dielectric coating to avoid excessive ink absorption and to reduce the surface roughness [10].

Manuscript received September 05, 2014; accepted October 09, 2014. Date of publication October 15, 2014; date of current version February 04, 2015. This work was supported by the Academy of Finland and the Finnish Funding Agency for Innovation.

H. Saghlatoon, T. Björninen, L. Sydänheimo, and L. Ukkonen are with Tampere University of Technology, 33720 Tampere, Finland (e-mail: toni.bjorninen@tut.fi; lauri.sydanheimo@tut.fi; leena.ukkonen@tut.fi).

M. M. Tentzeris is with the Georgia Institute of Technology, Atlanta, GA 30332-250 USA (e-mail: etentze@ece.gatech.edu).

Color versions of one or more of the figures in this letter are available online at http://ieeexplore.ieee.org.

Digital Object Identifier 10.1109/LAWP.2014.2363085

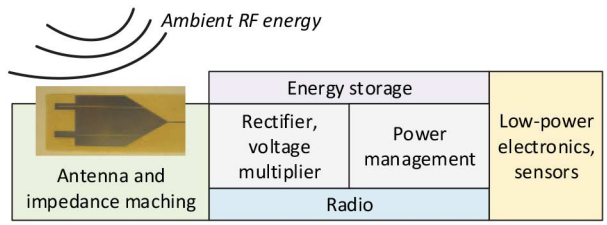

Fig. 1. Diagram of an ambient RF energy harvester.

II. Design Of The Wideband Harvester Antenna

A diagram of an ambient RF energy harvester is depicted in Fig. 1. Here, the antenna captures the electromagnetic energy present in ambient RF signals within a wide range of frequencies. Wideband antenna equivalent circuit model [11] combined with advanced circuit design techniques, such as resistance compression networks [12], can be used to interface the antenna to an RF front end. Printed supercapacitor [9] is a promising candidate for the integration of charge storage in a paper-based platform.

To exemplify the general design requirements for the harvester antenna, we considered P2110 Powercast Energy Harvesting Module for 600–1500-MHz band with a single-ended 50-Ω RF front end. It is capable to harvest energy from ultra-high-frequency (UHF) Digital TV, UHF RFID systems, and GSM 900, which are some of the strongest signals in this frequency range [8]. Taking into account that the incident energy arrives from an unspecified source, we considered a monopole to be a fit antenna type for the harvester. It does not include vias and is therefore simple to fabricate in an inkjet printing process. Moreover, it has an inherently omnidirectional radiation pattern for broad spatial coverage. Finally, it has a single-ended input so that it can be directly interfaced to the harvester module and capability to provide wide bandwidth through appropriate design, as detailed below.

Analysis of a rectangular planar monopole antenna shown in Fig. 2(a) can be based on a microstrip patch antenna with a ground plane at infinity. Referring to Fig. 2(a), the physical

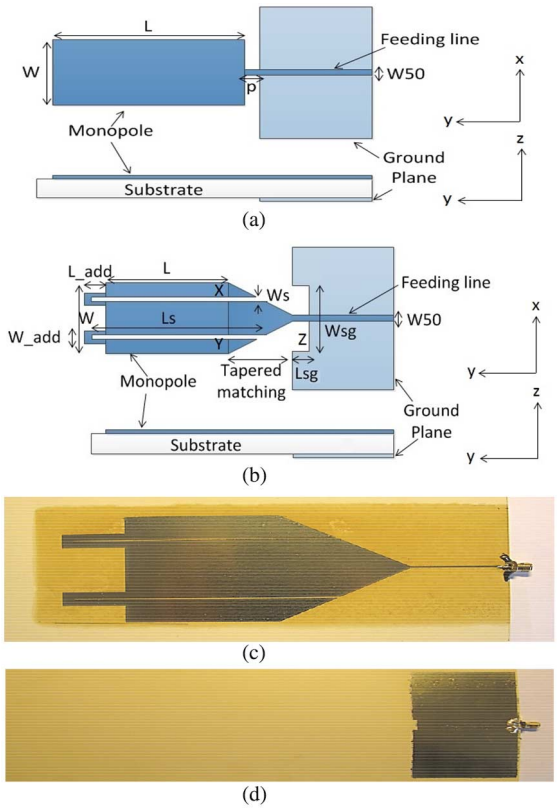

Fig. 2. (a) Geometry of a planar monopole antenna. (b) Geometry of the proposed wideband planar monopole antenna. (c) Top layer of the fabricated antenna. (d) Bottom layer of the fabricated antenna.

TABLE I
PROPERTIES OF THE SUBSTRATE AND PRINTED CONDUCTOR [14]

Relative Permittivity of cardboard	1.78
Loss tangent of cardboard	0.025
Thickness of cardboard	560 μm
Conductivity of silver ink	$2{\cdot}10^7$ S/m
Thickness of silver ink	3 μm

TABLE II
PHYSICAL DIMENSIONS OF THE ANTENNA IN MILLIMETERS

L	W	Tapered matching	W_{50}
70	70	60	1
L_S	W_S	L_{sg}	W_{sg}
66	1	2	10
L_{add}	W_{add}		
30	9		

dimensions to achieve a well-performing monopole antenna at the lowest operation frequency of f_l need to satisfy [13]

$$r = \frac{W}{2\pi} \quad \text{and} \quad f_l = \frac{7.2}{L + r + p} \tag{1}$$

where W is the width of the radiator (in centimeters), p is the gap between the ground plane edge and the radiator edge (in centimeters), L is the length of the radiator (in centimeters), and f_l is the lowest operation frequency (in gigahertz).

The dielectric loss in the substrate and the conductivity of the conductor predominantly affect the antenna radiation efficiency.

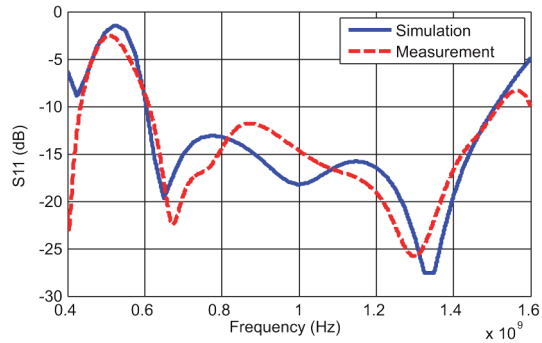

Fig. 3. Simulated and measured input reflection coefficient.

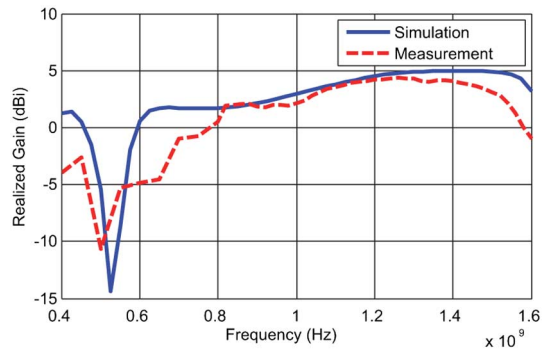

Fig. 4. Simulated and measured maximum realized gain.

Accurate knowledge of the thickness of the substrate and its dielectric constant are required in the design of the feeding line. Here, we refer to our earlier investigation [14] on the dielectric properties of the thin packaging cardboard from Stora Enso and the conductivity of Harima NPS-JL silver nanoparticle ink deposited on the cardboard after the same surface pretreatment that was used in the present work. The pretreatment will be further detailed in Section III. The acquired data is summarized in Table I. Based on this information, we computed the widths of the 50-Ω feedline (W_{50}) and the radiating element ($L+p$) to be 2 and 120 mm (quarter-wavelength), respectively, at the lowest frequency of the bandwidth: $f_l = 600$ MHz. The corresponding value for the width of the monopole (W) is 60 mm. Since parameter p has great influence on the input impedance of the antenna, the most suitable value was acquired through a parametric sweep. This value was used to find the most suitable width of the feeding line to achieve good impedance matching. The obtained dimensions of the rectangular monopole were used to initiate the design of the wideband antenna. The size of the ground plane was chosen to be as small as possible without compromising the efficiency of the antenna.

The bandwidth of a monopole antenna can be improved with various methods and their combination. First, we added a triangular tapered segment between the feedline and the radiating element. The added segment smoothened the transition between the radiator and the feeding line reducing reflections in this part [15]. Second, two slits defined by the parameters W_S, L_{add}, and W_{add} in Fig. 2(b) were cut into the radiating element to create a resonance at a lower frequency compared to the fundamental resonance of the monopole element. This way, the

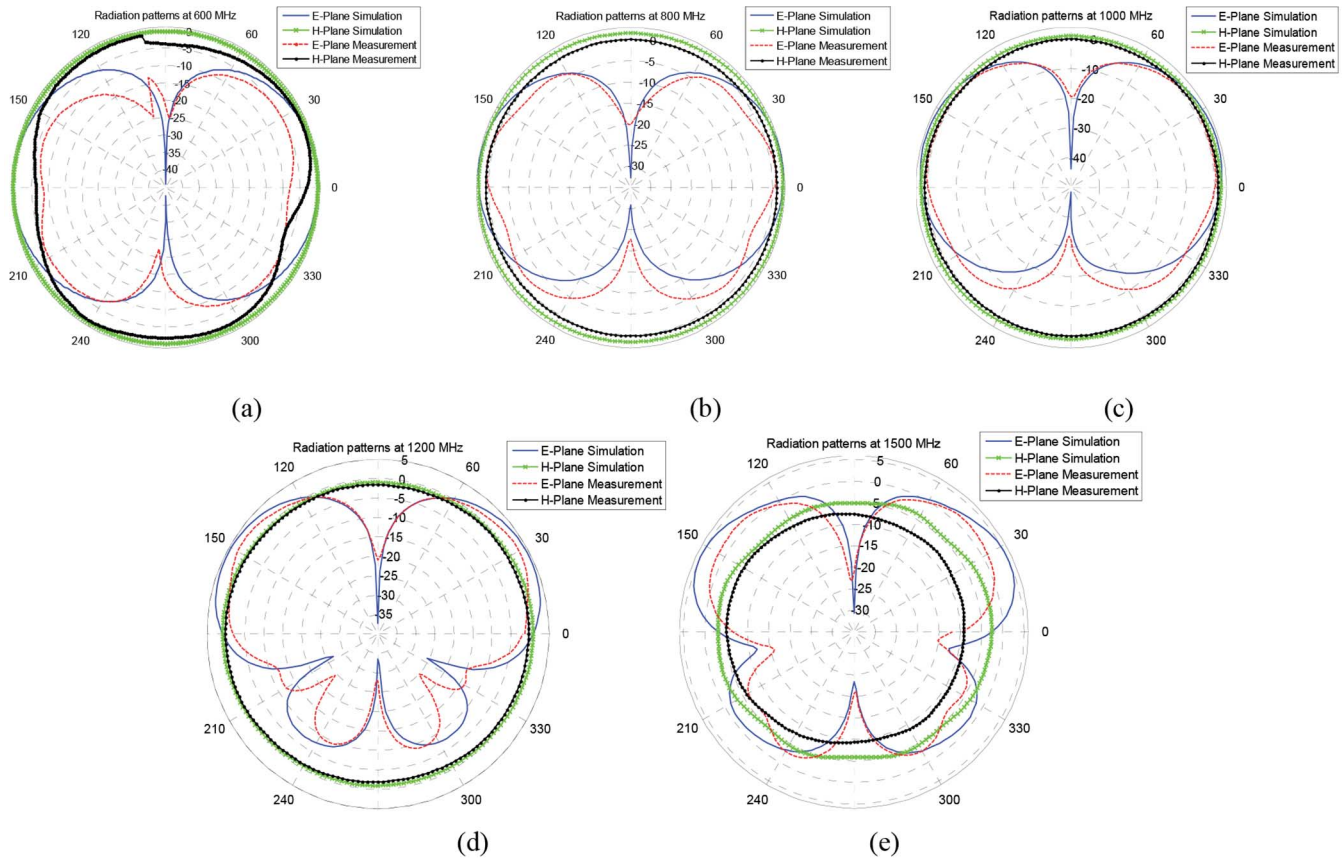

Fig. 5. Simulation and measurement results for the radiation patterns of the proposed antenna at different frequencies. (a) 600 MHz. (b) 800 MHz. (c) 1 GHz. (d) 1.2 GHz. (e) 1.5 GHz.

impedance bandwidth was further broadened. In addition, the ground plane was modified by cutting a slot defined by the parameters W_{sg} and L_{sg} in Fig. 2(b) into it. As established in [16] and [17], this creates a strategic perturbation in the current distribution, which manifested itself as further improvement in the impedance bandwidth. The geometry of the wideband monopole antenna is illustrated in Fig. 2(b). Table II presents the values of the optimized geometrical parameters.

III. Antenna Fabrication and Testing

We fabricated the wideband monopole antenna on thin packaging cardboard from Stora Enso using Dimatix DMP-2831 inkjet materials printer equipped with 10-pl printhead. First, to reduce the surface roughness and to prevent the penetration of ink into the substrate, we printed a thin dielectric coating on the cardboard. For this purpose, we deposited five layers of Primer (composed of tetrahydrofurfuryl acrylate, ethoxylated trimethylolpropane triacrylate, 2-hydroxy-2-methyl-1-phenyl-propan-1-one, and bis-phenylphosphineoxide and appropriate for surface pretreatment [10]) with 1016 dpi printing resolution. The print was cured after each printed layer with ultraviolet exposure for 15 min and then sintered for 1 h at 150° C.

In the following stage, we printed the antenna on the coated surface using Harima NPS-JL silver nanoparticle ink with 55.5 wt% metal content. To achieve high conductivity, we deposited eight layers of silver ink with 635 dpi printing resolution. The print was sintered for 1 h at 150° C after every two printed layers. This prevented the spreading of the ink and allowed us to build up subsequent conductive layers effectively. In our earlier investigation [14], we determined the conductivity of the printed layer to be $2 \cdot 10^7$ S/m, using the two-transmission-line method. The inkjet-printed wideband planar monopole antenna on cardboard is depicted in Fig. 2(c) and (d).

We used an Agilent PNA E8358A two-port vector network analyzer (VNA) to measure the antenna input reflection coefficient. As shown in Fig. 3, the measured result agreed with the simulations. To measure the realized gain, radiation patterns, and antenna efficiency $(\mathrm{e_A})$, we used primarily Satimo Starlab near-field antenna measurement system. It provides these data through a built-in near-to-far-field transformation. Furthermore, we used the measured S_11 to remove the impact of impedance mismatch from $(\mathrm{e_A})$ to obtain the radiation efficiency. Below 800 MHz, which was the lowest operable frequency of our near-field setup, we used a far-field measurement based on a standard gain horn to determine the realized gain and radiation pattern of the antenna.

Fig. 4 shows the simulated and measured realized gain of the antenna versus frequency. Due to the fact that the near-field measurement system is more accurate (peak gain accuracy between 0.8 and 1 GHz is ± 0.9 dB) compared to the far-field measurement (± 1.5 dB peak gain accuracy at 800 MHz plus the error in the alignment of the antennas and higher reflection levels), the results agreed well for the frequencies higher than

TABLE III
SIMULATED AND MEASURED RADIATION EFFICIENCY

Frequency (MHz)	800	1000	1200	1500
Simulation result	95.1%	94.9%	95.6%	92.6%
Measurement result	73.0%	78.6%	80.5%	72.6%

800 MHz. Between 600 and 800 MHz, we observed discrepancies, which were likely caused by multipath reflections due to the nonidealities of the anechoic chamber. However, at the lower frequencies a better agreement was found, and the simulated null near 500 MHz is also present in the measurement.

The simulated and measured radiation patterns at different frequencies are shown in Fig. 5. The results confirm that the antenna has an omnidirectional radiation pattern in the H-plane [xz-plane in Fig. 2(b)] throughout its operational frequency band from 600 MHz to 1.5 GHz. This is desirable in the power-harvesting application, where the incident energy arrives from an unspecified location. The radiation pattern in E-plane [yz-plane in Fig. 2(b)] exhibits an 8-shape similar to a dipole or a monopole with finite ground plane. At higher frequencies, beyond 1200 MHz, the effective length of the antenna increases, and thus sidelobes appeared [Fig. 5(d) and (e)]. Finally, Table III presents the simulated and measured radiation efficiency of the antenna at several frequencies throughout the studied bandwidth. The results show that the antenna achieved the measured radiation efficiencies from 72% to 80% throughout the wide bandwidth from 800 to 1200 MHz. This confirms that the studied antenna is a viable candidate for the wideband ambient RF energy-harvesting application. We expect that the simulation overestimated the radiation efficiency due to possible imperfections in the conductivity and uniformity of the printing outcome.

IV. CONCLUSION

Fabrication of antennas on low-cost environmentally-friendly materials bulk materials, such as paper and cardboard, is attractive for the development of future wireless platforms. We presented the design and inkjet-printing fabrication of a novel wideband planar monopole antenna for ambient RF energy harvesting in the 600–1500-MHz band. We printed both the dielectric coating and silver nanoparticle ink using a tabletop inkjet printer and achieved a highly conductive metallization on the fibrous and porous cardboard substrate providing higher than 72% measured radiation efficiency (800–1500 MHz). Overall, the simulated and measured results attested the electromagnetic performance of the antenna and proved it fit for the wideband ambient RF energy-harvesting application. The future work includes the integration of the antenna with a power management system and ultra-low-power sensors.

REFERENCES

[1] G. Shaker, S. Safavi-Naeini, and M. M. Tentzeris, "Inkjet printing of ultrawideband (UWB) antennas on paper-based substrates," *IEEE Antennas Wireless Propag. Lett.*, vol. 10, pp. 111–114, 2011.
[2] B. Shao, Y. Amin, Q. Chen, R. Liu, and L.-R. Zheng, "Directly printed packaging-paper-based chipless RFID tag with coplanar LC resonator," *IEEE Antennas Wireless Propag. Lett*, vol. 12, pp. 325–328, 2013.
[3] W. Pachler *et al.*, "A silver ink-jet printed UHF booster antenna on flexible substratum with magnetically coupled RFID die on-chip antenna," in *Proc. EuCAP*, 2013, pp. 1730–1733.
[4] W. R. Heinzelman, A. Chandrakasan, and H. Balakrishnan, "Energy-efficient communication protocol for wireless microsensor networks," in *Proc. HICSS*, Maui, HI, USA, 2000, pp. 1–10.
[5] T. Pering, Y. Agarwal, R. Gupta, and R. Want, "Coolspots: Reducing the power consumption of wireless mobile devices with multiple radio interfaces," in *Proc. MobiSys*, Uppsala, Sweden, 2006, pp. 220–232.
[6] M. Armand and J. M. Tarascon, "Building better batteries," *Nature*, vol. 451, no. 7179, pp. 652–657, Feb. 2008.
[7] N. Borges Carvalho *et al.*, "Wireless power transmission: R&D activities within Europe," *IEEE Microw. Theory Techn.*, vol. 62, no. 4, pp. 1031–1045, Apr. 2014.
[8] J. Tavares *et al.*, "Spectrum opportunities for electromagnetic energy harvesting from 350 MHz to 3 GHz," in *Proc. ISMICT*, Tokyo, Japan, 2013, pp. 126–130.
[9] S. Lehtimäki *et al.*, "Performance of printable supercapacitors in an RF energy harvesting circuit," *Int. J. Elect. Power Energy Syst.*, vol. 58, no. 2014, pp. 42–46, Jan. 2014.
[10] A. Denneulin, J. Bras, A. Blayo, and C. Neuman, "Substrate pre-treatment of flexible material for printed electronics with carbon nanotube based ink," *Appl. Surf. Sci.*, vol. 257, no. 8, pp. 3645–3651, Feb. 2011.
[11] D. Caratelli, R. Cicchetti, G. Bit-Babik, and A. Faraone, "Circuit model and near-field behavior of a novel patch antenna for WWLAN applications," *Microw. Opt. Technol. Lett.*, vol. 49, no. 1, Jan. 2007.
[12] K. Niotaki, A. Georgiadis, and A. Collado, "Dual-band rectifier based on resistance compression networks," in *Proc. IEEE MMT-S IMS*, Tampa Bay, FL, USA, 2014, pp. 1–3.
[13] G. Kumar and K. P. Ray, "Broadband planar monopole antennas," in *Broadband Microstrip Antennas*. Norwood, MA, USA: Artech House, 2003.
[14] H. Saghlatoon, L. Sydänheimo, L. Ukkonen, and M. M. Tentzeris, "Optimization of inkjet printing of patch antennas on low-cost fibrous substrates," *IEEE Antennas Wireless Propag. Lett.*, vol. 13, pp. 915–918, 2014.
[15] J. Jung, W. Choi, and J. Choi, "A small wideband microstrip-fed monopole antenna," *IEEE Microw. Wireless Compon. Lett.*, vol. 15, no. 10, pp. 703–705, Oct. 2006.
[16] A. A. Eldek, "Numerical analysis of a small ultra wideband microstrip-fed tap monopole antenna," *Prog. Electromagn. Res.*, vol. 65, pp. 59–69, 2006.
[17] M. Rajabi, M. Mohammadi, and N. Komjani, "Simulation of ultra wideband microstrip antenna using EPML-TLM," *Prog. Electromagn. Res. B*, vol. 2, pp. 115–124, 2008.